American Mineralogist, Volume 83, pages 36–42, 1998

An empirical model for the solubility of H_2O in magmas to 3 kilobars

GORDON MOORE,[1,]* TORSTEN VENNEMANN,[2] AND I.S.E. CARMICHAEL[1]

[1] Department of Geology and Geophysics, University of California, Berkeley, California 94720, U.S.A.
[2] Institut Geochemie, Wilhelmstrasse 56, D-72076, Tübingen, Germany

ABSTRACT

We present 16 new manometric determinations of H_2O solubility for a range of natural silicate liquid compositions equilibrated up to 3 kbar of H_2O pressure. As the threshold temperature of dehydration of the quenched glasses during measurements of the H_2O content becomes lower as a function both of bulk silicate composition and the dissolved H_2O content, we measured the H_2O released on heating over a range of temperature intervals. For example, alkali-rich samples having a dissolved H_2O content greater than ~6 wt% start to evolve H_2O at temperatures less than 150 °C, whereas more mafic samples and silicic samples with less than 6 wt% H_2O begin to dehydrate at temperatures greater than 200 °C. This behavior is consistent with the concept that alkali-rich liquids can have their glass transition temperatures lowered substantially by dissolved H_2O and that H_2O is released only significantly on heating in the supercooled liquid region, rather than in the glass region. Using these new data, in conjunction with previous data from the literature, we refined and extended the empirical H_2O solubility model of Moore et al. (1995b). The new model works well ($2\sigma = \pm 0.5$ wt%) between 700–1200 °C and 1–3000 bar and can be applied to any natural silicate liquid in that range. The model may also be used for systems where $X_{H_2O} < 1$ in the vapor phase.

INTRODUCTION

Dissolved H_2O in the silicate liquid portion of magmas is one of the most influential components of igneous systems. It affects the density, viscosity, and the phase equilibria of these systems (Burnham 1981; Schulze et al. 1997; Johnson et al. 1994; Lange 1994; Ochs and Lange 1997; Paillat et al. 1992), thereby determining their chemical and transport history as well as their eruptive behavior at the surface. As it is the exsolution of high H_2O contents (4–6 wt%; Sisson and Layne 1992; Anderson et al. 1989) that drives most explosive volcanic activity and controls the formation of magmatic ore fluids (e.g., Lowenstern 1994), it is clear that an understanding of the H_2O solubility in natural silicate liquids as a function of pressure, temperature, and melt composition is of paramount importance.

Much work has been done toward this end but past solubility measurements tended to focus on natural and synthetic granitic and feldspar liquid compositions at 2 to 8 kbars (Burnham and Davis 1971; Burnham and Jahns 1962; Dingwell et al. 1984; Holtz et al. 1992; Oxtoby and Hamilton 1978) or on single natural compositions at low pressures relevant to magmatic degassing processes (Blank et al. 1993; Dixon et al. 1995; Silver et al. 1990). None of these studies provided the means to predict the effect of bulk composition on H_2O solubility in natural silicate liquids, though there were several attempts to model the available data. These studies were hampered however by either the lack of data (Nicholls 1980) or by the significant amount of scatter that is found in the literature (Papale 1997). For example, the data of Hamilton et al. (1964) provided the first information on the H_2O solubilities for a range of natural compositions (basalt to andesite) at varying *P-T* conditions. These early measurements are problematic however as they used a weight-loss method to determine H_2O content, and this method is subject to error because of H_2O trapped in vesicles. Furthermore, the liquid may have lost H_2O on quench because they used a relatively slow quenching method. Despite these problems their study stands as the benchmark for any estimate of H_2O solubility in naturally occurring silicate liquids, but it is also representative of the types of experimental error present in the earlier solubility studies.

More recent H_2O solubility measurements on a range of natural melt compositions to 2 kbars were conducted by Moore et al. (1995b) using a vacuum extraction method to measure H_2O content, as well as a rapid quench synthesis technique, in an effort to eliminate the problems encountered by Hamilton et al. (1964). These experiments were conducted over a wide range of *P-T* conditions and on many lava compositions to constrain an empirical model for H_2O solubility as a function of melt composition, temperature, and pressure. Although the Moore et al. (1995b) model worked well for most lava composi-

---

* Present address: Department of Geology, Arizona State University, Tempe, AZ 85287, U.S.A.

0003–004X/98/0102–0036$05.00

TABLE 1. Starting material compositions

	Mas-49 augite minette	Mas-22 basaltic andesite	Mas-12 andesite	TC-19 phonolite	442 biotite trachyte	20421 leucitite	NZC-4 peral-kaline rhyolite	87S35 basalt	TT152-21-35 tholeiite	DC-1 rhyolite	KS rhyolite	203, 205 basalt	A9, A14 andesite	CAM-73 rhyolite
SiO_2	53.6	55.3	62.6	59.3	56.3	46.9	71.8	50.6	50.8	76.6	77.5	50.71	58.41	75.0
TiO_2	1.76	0.74	0.63	0.69	1.70	1.10	0.24	1.27	1.84	0.10	—	1.70	1.15	0.07
Al_2O_3	13.8	17.4	17.3	19.2	18.1	20.91	9.7	19.1	13.7	12.7	12.5	14.48	18.25	12.29
Fe_2O_3	4.80	1.96	2.01	1.01	2.02	2.99	1.80	3.74	—	0.58	—	4.89	1.50	0.33
FeO	1.62	4.22	2.01	2.37	3.20	3.26	3.97	5.33	12.4*	0.56	1.0*	9.07	4.96	0.71
MnO	0.09	0.12	0.06	0.19	0.14	0.20	0.14	0.17	0.22	—	—	0.22	0.10	0.05
MgO	5.34	6.68	2.65	0.44	1.68	1.28	0.01	4.32	6.67	0.02	—	4.68	3.39	0.04
CaO	6.85	7.28	5.64	0.86	4.10	4.33	0.20	8.85	11.5	0.31	0.5	8.83	6.70	0.58
Na_2O	3.33	3.97	4.05	9.80	5.42	6.90	5.30	4.23	2.68	4.1	3.6	3.16	4.35	4.03
K_2O	6.27	1.18	1.61	5.84	5.94	9.15	4.47	1.00	0.15	4.6	4.8	0.77	0.82	4.66
P_2O_5	1.37	0.27	0.24	0.10	0.58	0.41	0.02	0.37	0.22	—	—	0.36	0.26	—
Total	98.8	99.1	98.8	99.8	99.2	97.4	97.6	98.9	100.2	99.6	99.9	98.9	99.9	97.8

Notes: Mas-49, Mas-22, Mas-12, TC-19, 442, and 20421, are wet chemical analyses by I.S.E. Carmichael; NZC-4 is probe analysis from Moore et al. (1995a); 87S35 is from Sisson and Grove (1993); TT152-21-35 is from Dixon et al. (1995); DC-1 is from Shaw (1963); KS is from Silver et al. (1990); 203, 205, and A9, A14 are from Hamilton et al. (1964); TC-19 is same phonolite composition used by Carroll and Blank (1997).

* Total iron as FeO.

tions, particularly the calc-alkaline series, the present study represents a significant refinement because it presents new solubility data to 3 kbars of pressure (H_2O contents up to ~10 wt%) and documents the degassing behavior of silicate glass samples with high H_2O contents (>6 wt%) that is significant to the manometric method used in determining the H_2O solubility. Solubility data for several new liquid compositions (e.g., phonolite and high-alumina basalt) are also presented that extend the compositional range covered by the experiments. These new observations and data are used in conjunction with data from the literature to regress new coefficients for the same model equation as Moore et al. (1995b), resulting in a simple empirical expression for dissolved H_2O content that can be used on any lava composition up to 3 kbars.

EXPERIMENTAL TECHNIQUE

Samples were equilibrated for 48 h under H_2O-saturated conditions (Table 1) in an internally heated pressure vessel with a rapid quench assembly (Holloway et al. 1992). The pressure medium was a 0.1 vol% hydrogen and 99.9 vol% argon gas mixture that maintains an f_{O_2} of about two log units above the nickel-nickel oxide buffer within the vessel (Moore et al. 1995a). Approximately 100 mg of rock powder, plus the minimum amount of H_2O needed to saturate the liquid and maintain a vapor phase, were loaded into a $Ag_{70}Pd_{30}$ capsule to minimize Fe loss. After quenching and verifying that a fluid phase was present, fragments of the quenched glass were used for H_2O content determination and for electron microprobe analysis to verify that the composition of the liquid had not changed during the experiment or that quench crystals had formed. Microprobe analyses were done at University of California, Berkeley, using operating conditions to minimize volatile loss (10 nA beam current, 20 μm beam diameter). If quench crystals were found or the capsule leaked the experiment was thrown out and not analyzed. The samples often contained vesicles, particularly the silicic compositions, and were rarely bubble-free. The vesicles were always oblong in appearance, suggesting they were convecting during equilibration and are not due to exsolution during quench.

Samples for analysis of their H_2O content were gently crushed under ethanol to ~350 μm to aid in devolatilization of the glass, minimize adsorbed H_2O (Newman et al. 1986), and to eliminate free H_2O trapped in vesicles. They were then loaded onto an extraction line and evacuated to $<10^{-8}$ bar at room temperature for 12 h. H_2O was then extracted at various temperatures according to a method modified after Vennemann and O'Neil (1993). A small resistance furnace was used for temperatures up to 820 °C with the temperatures monitored with a calibrated K-type thermocouple in contact with the 7 mm o.d. silica tube containing the sample. For temperatures in excess of 1400 °C the samples were heated in the silica tube with an oxygen-propane torch.

To better understand the dehydration behavior of our samples, H_2O release spectra were obtained for several select samples by holding the samples at a fixed temperature in the vacuum line until the sample no longer dehydrated (about 2 h at the 50 and 150 °C steps, 3 to 4 h at the 300 and 420 °C steps, 2 h at the 800 °C step, and about 10 min at the >1400 °C step). H_2O was removed continuously from the sample and extracted before the next step. These data are given in Table 3. Thermal gravimetric data were also collected for a H_2O rich andesite sample (PEM12-4) on a Shimadzu thermal gravimetric analyzer (TGA) using 50 °C steps with a 15 min holding and ramping interval.

RESULTS

Low-temperature dehydration of silicate glasses with high H_2O contents

Newman et al. (1986) established that a significant amount of adsorbed water is found in rhyolite glass

TABLE 2. Experimental data used in regression

Sample no.	P (bars)	T (°C)	H_2O melt (wt%)	X_{H_2O} (melt)	f_{H_2O} (vapor)
SAT-M12-1*	703	1100	2.62	0.087	685
SAT-M12-2*	1865	1100	5.03	0.155	1815
SAT-M12-4†	2985	1050	6.76	0.198	2909
PE-M12-20†	2830	1000	6.82	0.199	2683
SAT-M22-1*	1930	1100	5.06	0.153	1881
SAT-M22-3*	1113	1100	2.37	0.082	639
SAT-M22-4†	3110	1100	6.37	0.185	3171
SAT-M22-5†	2896	1100	6.59	0.190	2922
SAT-TC19-3*	655	1100	2.37	0.082	639
SAT-TC19-7†	3027	900	8.70	0.244	2655
SAT-TC19-8†	1944	900	7.30	0.213	1675
R105‡	360	900	2.40	0.080	344
R116‡	560	875	3.00	0.101	560
SAT-442-4†	3013	1050	6.43	0.195	2971
SAT-442-5†	1982	1100	5.40	0.169	1934
SAT-20421-2*	1075	1180	2.68	0.096	1063
SAT-NZC4-4*	1470	1000	5.23	0.159	1363
SAT-NZC4-9†	2841	900	8.00	0.225	2475
SAT-NZC4-11†	1986	900	6.34	0.187	1711
SAT-M49-2*	1280	1130	4.55	0.143	1251
SAT-M49-3*	814	1130	3.41	0.111	797
17H§	717	1200	2.56	0.082	711
20H§	310	1200	1.74	0.057	308
21H§	507	1200	2.42	0.078	503
SAT-87S35-1†	2117	1100	4.51	0.140	2091
SAT-87S35-3†	2185	1050	4.65	0.149	2112
SAT-87S35-4†	2206	1050	5.43	0.164	2074
SAT-87S35-5†	2916	1050	6.40	0.186	2863
PDIKS110#	190	850	1.46	0.050	184
PDIKS102#	500	850	3.15	0.102	463
PDIKS115#	980	850	3.94	0.124	857
PDIKS111#	1470	850	5.06	0.154	1238
PDIKS113#	1260	850	4.43	0.137	1075
Shaw, 1kb‖	1000	900	4.3	0.134	898
Shaw, 2kb‖	2000	800	6.2	0.183	1565
SAT-CAM73-6†	2827	900	8.36	0.233	2462
SAT-CAM73-7†	1848	900	6.34	0.194	1594
205**	6067	1100	9.4	0.255	7687
A14**	5309	1100	10.1	0.267	6303
203**	3000	1100	5.93	0.117	3041
A9**	3000	1100	7.4	0.211	3041

* Moore et al. 1995a.
† This study.
‡ Carroll and Blank 1997.
§ Dixon et al. 1995.
# Silver et al. 1990.
‖ Shaw 1963.
** Hamilton et al. 1964.

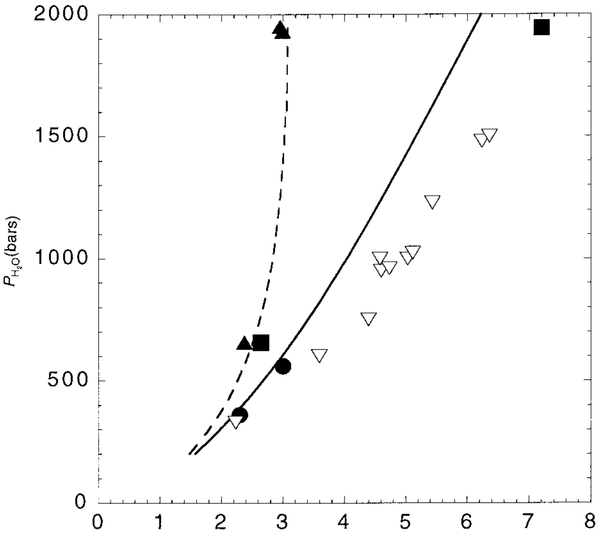

FIGURE 1. Comparison of Moore et al. (1995b) data for phonolite (solid triangles) with the data of Carroll and Blank (1997) (IR = upside-down open triangles; manometry = solid circles, 850–900 °C) and the new data from this study (solid squares = 900 °C). The dashed line is the predicted H_2O solubility from Moore et al. (1995b), and the solid line is from this study calculated for 900 °C. Note the severe underestimation of the Moore et al. (1995b) data and its subsequent effect on their model curve.

samples with low dissolved H_2O content (<2 wt%), and therefore steps must be taken during the manometric procedure to rid the sample of this extraneous water (see above). Their solution, which became standard practice, was to heat the samples at about 150–200 °C under vacuum for 12 h using an inductance furnace, then raise the temperature and commence the manometry measurement. Moore et al. (1995b) used a similar technique for their samples, which contained up to ~6 wt% H_2O, except where the samples were heated with a resistance furnace as described above. Comparison of the Moore et al. (1995b) data for a phonolite (TC-19) at 2 kbar water pressure with the IR solubility data of Carroll and Blank (1997) on the identical lava shows that the Moore et al. (1995b) data and subsequent model greatly underestimate the H_2O solubility of this composition (Fig. 1).

To further investigate the low manometry results on the phonolite and to better understand the dehydration behavior of natural silicate glasses, several H_2O release ma-

TABLE 3. Manometric water release data (wt% H_2O)

Sample no.	50 °C	150 °C	200 °C	300 °C	420 °C	800 °C	820 °C	1400 °C
SAT-CAM73-6	0.60	2.25		3.08	1.50	0.97		0.10
SAT-CAM73-7	0.11	1.10		2.92	1.46	1.09		0.11
SAT-87S35-1			0.19				4.44	0.12
SAT-87S35-5	0.03	0.09		1.18	1.78	3.42		0.05
SAT-TC19-7			5.09				3.59	0.26
SAT-TC19-8	0.08	2.04		2.83	1.57	0.85		0.07
SAT-NZC4-9	0.65	3.40		2.01	1.50	0.73		0.07
SAT-NZC4-11	0.06	1.27		2.98	1.54	0.68		0.06
SAT-442-4	0.05	0.63		1.83	1.07	0.97		0.03
SAT-442-5	0.04	0.50		1.82	1.81	1.43		0.05

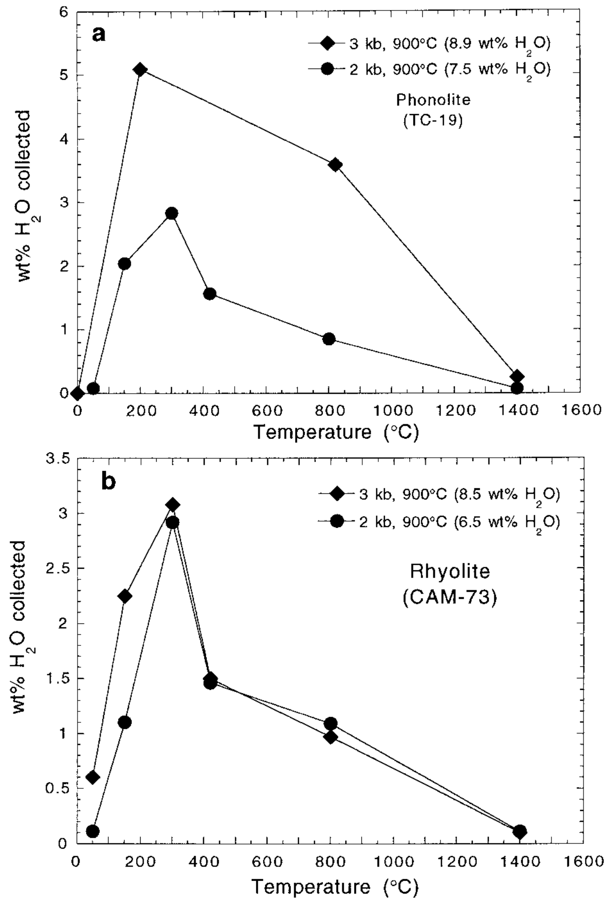

FIGURE 2. (**a**) H_2O release spectra for phonolite (TC-19). Note the significant amount of H_2O released below 200 °C. (**b**) H_2O release spectra for rhyolite (CAM-73) that shows similar behavior to the phonolite.

nometry experiments were conducted on selected samples (Table 3; Figs. 2 and 3). As illustrated in Figure 2, significant amounts of primary dissolved H_2O are released from the sample before 200 °C for the silica and alkali-rich samples with at least ~6 wt% dissolved H_2O. In contrast, Figure 3 shows the release spectra for a high alumina basalt, as well as thermal gravimetric data for an andesite, and establishes that dehydration does not begin until about 300 °C and peaks at about 800 °C for these compositions. This behavior suggests that the commencement of dehydration in silicate liquids is a function of both the bulk composition and the melt H_2O content. This is consistent with the work of Ochs and Lange (1997) who showed that albite glass does not dehydrate until it has gone through the glass transition because of kinetic effects. Therefore, as the H_2O content or the silica or alkali content of the glass increases, the glass transition temperature becomes lower as does the initial temperature of dehydration. Preliminary heat capacity measurements of silicic, H_2O-rich samples done on a scanning calorimeter show that these samples pass through their glass transition at temperatures less than 100 °C (Jean Tangemann, personal communication), which is consistent with the H_2O release data.

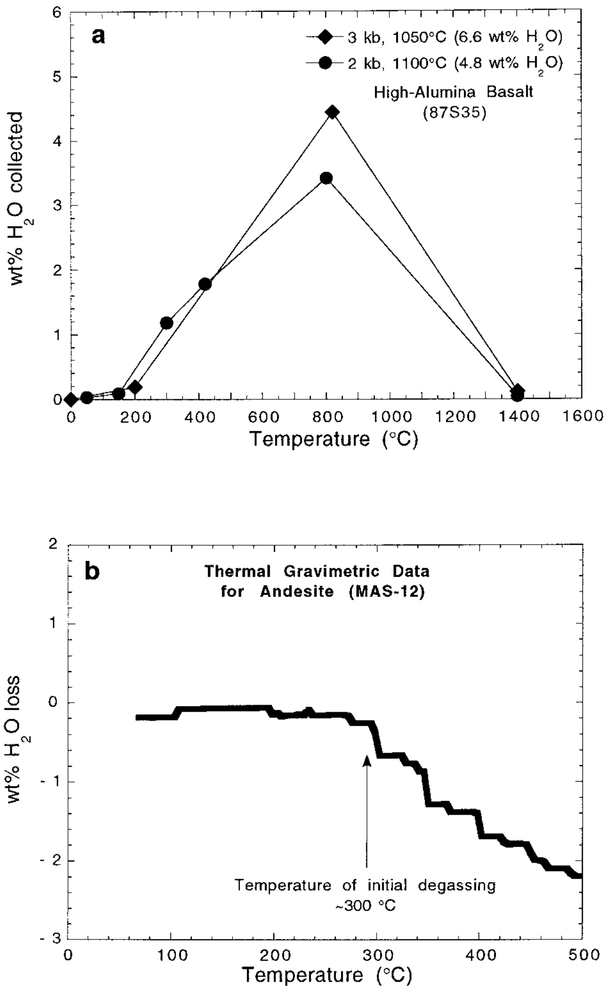

FIGURE 3. (**a**) H_2O release spectra for high alumina basalt (87S35A). Note that dehydration does not begin until temperatures are greater than 200 °C and that the H_2O release does not peak until ~800 °C. (**b**) Thermal gravimetry curve for andesite (Mas-12). Note that the sample does not lose significant weight (devolatilizes) until ~300 °C.

Subsequent to the discovery of this low-temperature dehydration behavior in H_2O -rich glasses, certain experiments of Moore et al. (1995a) became suspect, particularly the high-H_2O content experiments, as well as the alkali-rich and silica-poor compositions (e.g., 442, 20421, TC-19, and NZC-4). For this study, the suspect experiments were either redone or were excluded from the database (Table 2). Because of the high trace element concentrations (particularly Li_2O) in the pegmatitic composition of Burnham and Jahns (1962), which are not accounted for in our regression, we have also eliminated those data from the database. New experiments were also conducted at 3 kbar on a range of compositions and their H_2O solubilities were measured (Table 2) using the H_2O release spectra method, which eliminated the preliminary

TABLE 4. Model coefficients

Coefficient	Value	Standard error
a	2565	362
$b_{Al_2O_3}$	−1.997	0.706
b_{FeOt}	−0.9275	0.394
b_{Na_2O}	2.736	0.871
c	1.171	0.069
d	−14.21	0.54

Notes: N = 41; $R^2 = 0.97$; 1σ error = 0.148 for $2 \ln X^{melt}_{H_2O}$.

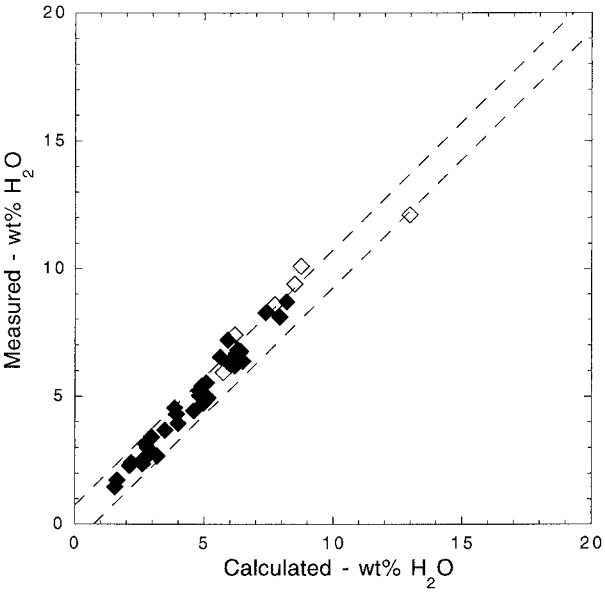

FIGURE 4. Measured vs. calculated H_2O solubility using Equation 1. Solid symbols include data from the literature and this study. Open symbols are the high-pressure data from Hamilton et al. (1964). Dashed lines represent the $\pm 2\sigma$ of the fit.

bake-out at 150–200 °C and the ensuing loss of dissolved H_2O that occured. Because adsorbed water is a function of surface area of the crushed glass samples, we assumed that each sample has 0.20 wt% adsorbed water, which is a maximum value derived from the H_2O release data below 300 °C on the high alumina basalt samples (87S35; Table 3).

Form of the model equation

The ultimate goal of this study is to develop a simple empirical expression that describes the dependence of H_2O solubility on temperature, pressure, and composition of the liquid. Therefore, for the reaction: H_2O (vapor) = H_2O (melt) we used the modified database from Moore et al. (1995b) in conjunction with the new data at 3 kbar (Table 2), to calibrate an equation of the form:

$$2 \ln X^{melt}_{H_2O} = \frac{a}{T} + \sum_i b_i X_i \left(\frac{P}{T}\right) + c \ln f^{fluid}_{H_2O} + d \qquad (1)$$

where $X^{melt}_{H_2O}$ = mole fraction of H_2O dissolved in the melt, $f^{fluid}_{H_2O}$ = fugacity of H_2O in the fluid, = temperature (Kelvin), = pressure (bars), = anhydrous mole fractions of the oxide components, and are the fit parameters (values in Table 4). The fugacity of H_2O in the fluid is calculated by using a modified Redlich-Kwong equation of state (Appendix of Holloway and Blank 1994). The mole fractions of the oxide components are calculated from the initial compositions (Table 1). As was discussed in Moore et al. (1995b), each term in Equation 1 can be identified with certain thermodynamic variables. Thus the a coefficient is related to the enthalpy of reaction for H_2O dissolved in the melt. No compositional dependence was found for this term, and it is in agreement with the enthalpies calculated by Silver et al. (1990). The b_i term is related to the molar volume of H_2O within the melt, and a significant compositional dependence was found for this variable, making it necessary to modify it with the statistically significant compositional terms. This compositional dependence is consistent with calculated values for basalt (Dixon et al. 1995), rhyolite, and albite (Lange 1994; Silver et al. 1990). The coefficient c reflects the observation that although $\ln X^{melt}_{H_2O}$ is linear with $\ln f^{fluid}_{H_2O}$, it has a slightly different slope for each liquid. The constant d can be related to the entropy of reaction and is significantly negative for the reaction as written.

Using an unweighted multiple linear regression for the data (initial compositions listed in Table 1; experiment conditions and H_2O contents are given in Table 2) the overall fit to the data is good (the coefficients and their standard errors are given in Table 4). Figure 4 shows the measured solubility values of the experiments vs. the calculated values. Two times the standard error of the regression is equal to ±0.5 wt% H_2O (dashed lines, Fig. 4), and this recalls that the error in a replicate determination is ±0.2 wt% H_2O (Moore et al. 1995b). Comparison of the model parameters of this regression with those of Moore et al. (1995b) show that the a, c, and d coefficients (which account for 90% of the variation in the data set) are the same within error. The most significant difference is that the compositional terms for the oxides have changed, reflecting the higher contents of H_2O in the alkali-rich samples. The b_i term of Moore et al. (1995b) was modified by the mole fraction of SiO_2, Al_2O_3, FeO_t, and CaO. With the new regression, SiO_2 became insignificant and CaO was replaced by Na_2O. Also, Moore et al. (1995b) found it necessary to weigh the high-pressure data of Hamilton et al. (1964) and Burnham and Jahns (1962) to acheive a more balanced distribution of the data. The new high pressure data of this study eliminates the need for this weighing, and the new model recovers the results of Hamilton et al. (1964) quite well (Fig. 4). An Excel-based spreadsheet that uses Equation 1 and the new coefficients is available on request from the first author.

Applications of the model equation for water solubility in natural silicate melts

The solubility curves for basaltic and rhyolitic composition, calculated using Equation 1 (Fig. 5) and solu-

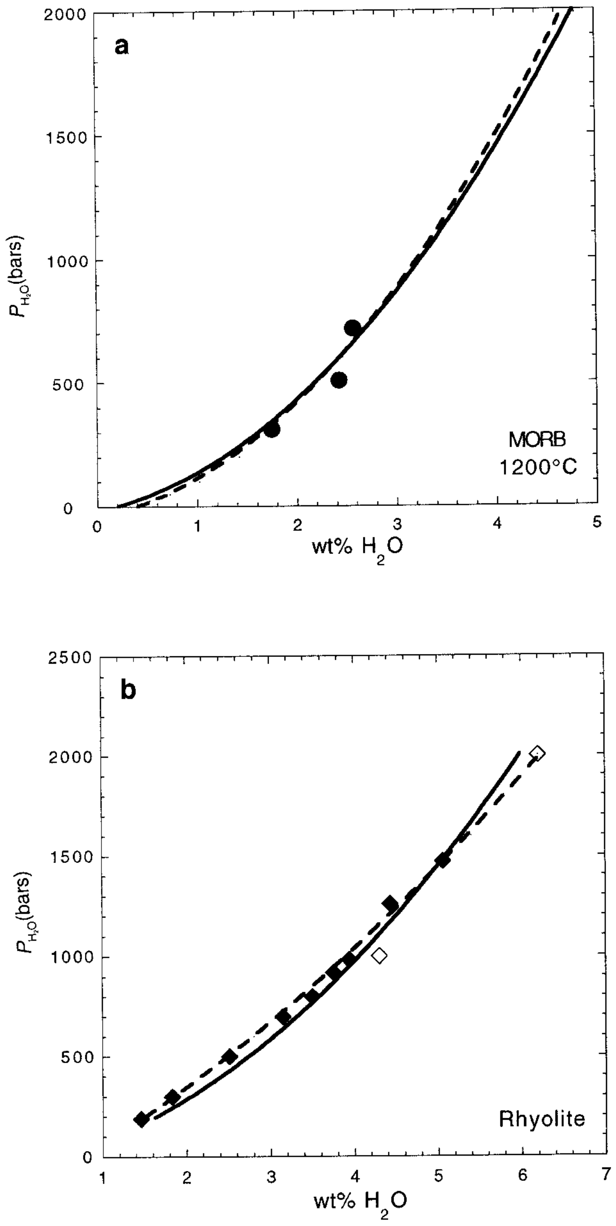

FIGURE 5. (**a**) Comparison of H_2O solubility models for MORB at 1200 °C. Data are from Dixon et al. (1995), as is the dashed curve. The solid line is from Equation 1. (**b**) Comparison of H_2O solubility models for rhyolite at 850 °C. Data are from Silver et al. (1990) and Shaw (1963). Dashed line is predicted curve from Silver et al. (1990). Solid line is from Equation 1.

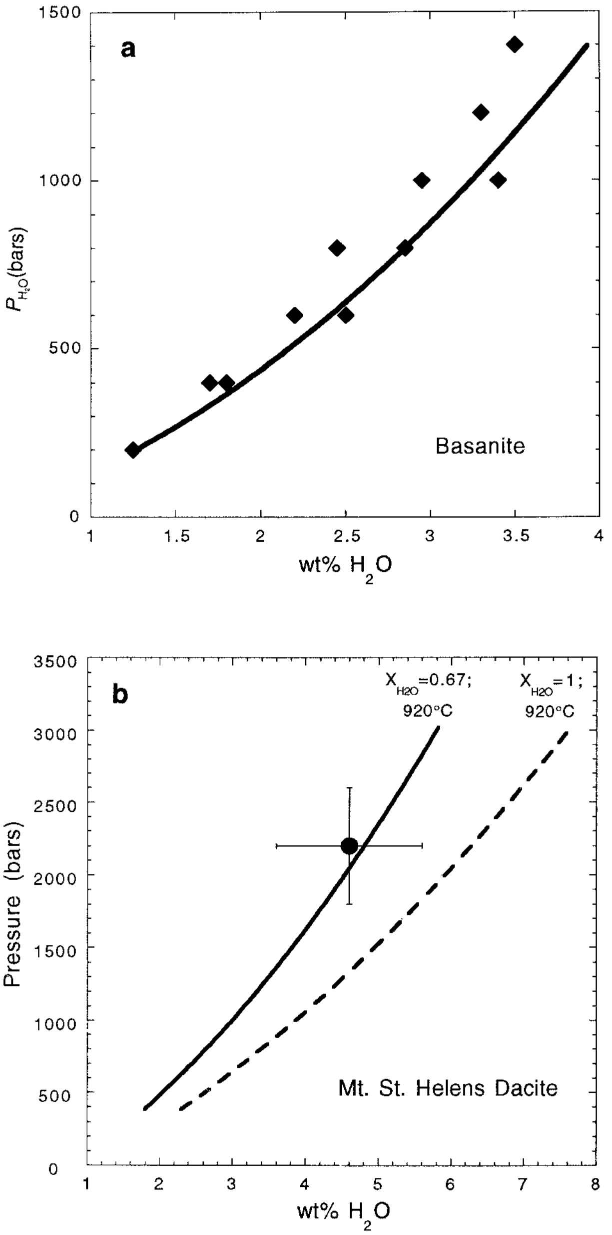

FIGURE 6. (**a**) Comparison of basanite H_2O solubility data at 1200 °C of Cocheo and Holloway (1994) (solid symbols) and Equation 1. Note that the basanite composition is not in the regressed database. (**b**) A comparison with the experimentally determined equilibrium conditions for the Mount St. Helens dacite (solid symbol) from Rutherford et al. (1985) and the predicted H_2O contents using Equation 1.

bility models presented by Dixon et al. (1995) and Silver et al. (1990), respectively, are indistinguishable. Both of these data sets are in our regression, however, so a better test is a composition not used in the calibration of our model and for which the equilibrium conditions and fluid composition are well known.

The H_2O solubility data for a basanitic composition (Holloway and Blank 1994) and the curve calculated using Equation 1 are shown in Figure 6a; our model appears to extrapolate well with changes in composition. Because Equation 1 contains a term involving the fugacity of H_2O vapor, it is also possible to calculate H_2O contents for liquids in equilibrium with a fluid phase that is not pure H_2O. For example, volcanic systems commonly have a significant fraction of CO_2 present in the fluid phase, thereby lowering the fugacity of H_2O (Anderson et al.

1989). So another test of our model is to predict H_2O contents of magmas for which temperature, pressure, and H_2O content are known either by direct measurement of melt inclusions or by experimental phase equilibria. This type of information is known only for a few cases, a good example being the dacite from the 1980 eruption of Mount St. Helens (Fig. 6b), where feldspar equilibria indicate $X^{\mathrm{fluid}}_{\mathrm{H_2O}}$ (Rutherford et al. 1985; Rutherford and Devine 1988). Using the residual glass composition to calculate the H_2O content at the appropriate conditions, it is apparent that our model is in good agreement with this estimate for the erupted dacite.

As the model appears to work for most natural igneous systems, it can also be applied to estimate the H_2O content in any liquid of known composition in experimental phase equilibria experiments. Moore and Carmichael (1998) did this for a series of andesite and basaltic andesite experiments conducted at H_2O-saturated conditions and documented the evolution of H_2O solubility in the liquid with increasing crystallization for both compositions.

Because this model results from an empirical regression, we caution against extrapolating it beyond the range of the data (up to ~3 kbar for any composition). Prediction to higher pressures is also problematic because of the complexities of critical behavior, as illustrated for albite liquids by the experiments of Paillat et al. (1992).

ACKNOWLEDGMENTS

This research was supported by National Science Foundation (grant EAR-9418105) to I.S.E. Carmichael. We thank Rebecca Lange for helpful comments and Mike Carroll and Malcolm Rutherford for thorough and constructive reviews. We especially thank Mike Carroll and Jen Blank for access to previously unpublished data and Jean Tangemann for measuring T_gs for several H_2O-rich glasses.

REFERENCES CITED

Anderson, A.T. Jr., Newman, S., Williams, S.N., Druitt, T.H., Skirius, C., and Stolper, E. (1989) H_2O, CO_2, Cl, and gas in plinian and ash-flow bishop rhyolite. Geology, 17, 221–225.

Blank, J.G., Stolper, E.M., and Carroll, M.R. (1993) Solubilities of carbon dioxide and water in rhyolitic melt at 850 °C and 750 bars. Earth and Planetary Science Letters, 119, 27–36.

Burnham, C.W. (1981) The nature of multicomponent aluminosilicate melts. In D.T. Rickard and F.E. Wickman, Eds., Chemistry and geochemistry of solutions at high temperatures and pressures, p. 197–229. Pergamon Press, New York.

Burnham, C.W. and Davis, N.F. (1971) The role of H_2O in silicate melts: 1. P-V-T relations in the system $NaAlSi_3O_8$-H_2O to 10 kilobars and 1000 °C. American Journal of Science, 270, 54–79.

Burnham, C.W. and Jahns, R.H. (1962) A method for determining the solubility of water in silicate melts. American Journal of Science, 260, 721–745.

Carroll, M.R. and Blank, J.G. (1997) The solubility of H_2O in phonolitic melts. American Mineralogist, 82, 549–556.

Dingwell, D.B., Harris, D.M., and Scarfe, C.M. (1984) The solubility of H_2O in melts in the system SiO_2-Al_2O3-Na_2O-K_2O at 1 to 2 kbar. Journal of Geology, 92, 387–395.

Dixon, J.E., Stolper, E.M., and Holloway, J.R. (1995) Experimental study of water and carbon dioxide solubilities in mid-ocean ridge basaltic liquids. Part I: Calibration and solubility models. Journal of Petrology, 36, 1607–1631.

Hamilton, D.L., Burnham, C.W., and Osborn, E.F. (1964) The solubility of water and effects of oxygen fugacity and water content on crystallization in mafic magmas. Journal of Petrology, 5, 21–39.

Holloway, J.R. and Blank, J.G. (1994) Application of experimental results to C-O-H species in natural melts. In Mineralogical Society of America Reviews in Mineralogy, 30, 187–230.

Holloway, J.R., Dixon, J.E., and Pawley, A.R. (1992) An internally heated, rapid-quench, high-pressure vessel. American Mineralogist, 77, 643–646.

Holtz, F., Behrens, H., Dingwell, D.B., and Taylor, R.P. (1992) Water solubility in aluminosilicate melts of haplogranite composition at 2 kbar. Chemical Geology, 96, 289–302.

Johnson, M.C., Anderson, A.T., and Rutherford, M.J. (1994) Pre-eruptive volatile contents of magmas. In Mineralogical Society of America Reviews in Mineralogy, 30, 281–330.

Lange, R.A. (1994) The effect of H_2O, CO_2 and F on the density and viscosity of silicate melts. In Mineralogical Society of America Reviews in Mineralogy, 30, 331–369.

Lowenstern, J.B. (1994) Dissolved water concentrations in an ore-forming magma. Geology, 22, 893–896.

Moore, G. and Carmichael, I.S.E. (1998) The hydrous phase equilibria (to 3 kbar) of an andesite and basaltic andesite from Western Mexico: Constraints on water content and conditions of phenocryst growth. Contributions to Mineralogy and Petrology, in press.

Moore, G., Righter, K., and Carmichael, I.S.E. (1995a) The effect of dissolved water on the oxidation state of iron in natural silicate liquids. Contributions to Mineralogy and Petrology, 120, 170–179.

Moore, G., Vennemann, T., and Carmichael, I.S.E. (1995b) The solubility of water in magmas to 2 kbar. Geology, 23, 1099–1102.

Newman, S., Stolper, E.M., and Epstein, S. (1986) Measurement of water in rhyolitic glasses: Calibration of an infrared spectroscopic technique. American Mineralogist, 71, 1527–1541.

Nicholls, J. (1980) A simple thermodynamic model for estimating the solubility of H_2O in Magmas. Contributions to Mineralogy and Petrology, 74, 211–220.

Ochs, F. and Lange, R. (1997) The partial molar volume, thermal expansivity, and compressibility of H_2O in $NaAlSi_3O_8$ liquid: New measurements and an internally consistent model. Contributions to Mineralogy and Petrology, in press.

Oxtoby, S. and Hamilton, D.L. (1978) Solubility of water in melts of the Na_2O-Al_2O_3-SiO_2 and K_2O-Al_2O_3-SiO_2 systems. Progress in experimental petrology. National Environmental Research council, 4, 33–36.

Paillat, O., Elphick, S.C., and Brown, W.L. (1992) The solubility of water in $NaAlSi_3O_8$ melts: A re-examination of Ab-H_2O phase relationships and critical behavior at high pressures. Contributions to Mineralogy and Petrology, 112, 490–500.

Papale, P. (1997) Thermodynamic modeling of the solubility of H_2O and CO_2 in silicate liquids. Contributions to Mineralogy and Petrology, 126, 237–251.

Rutherford, M.J. and Devine, J.D. (1988) The May 18, 1980, eruption of Mount St. Helens: 3. Stability and chemistry of amphibole in the magma chamber. Journal of Geophysical Research, 93, 11949–11959.

Rutherford, M.J., Sigurdsson, H., Carey, S., and Davis, A. (1985) The May 18, 1980, eruption of Mount St. Helens: Melt composition and experimental phase equilibria. Journal of Geophysical Research, 90, 2929–2947.

Schulze, F., Behrens, H., Holz, F., Ruox, J., and Johannes, W. (1997) The influence of H_2O on the viscosity of a haplogranitic melt. American Mineralogist, 81, 1155–1165.

Shaw, H.R. (1963) Obsidian-H_2O viscosities at 1000 and 2000 bars in the temperature range 700 to 900 °C. Journal of Geophysical Research, 68, 6337–6343.

Silver, L.A., Ihinger, P.D., and Stolper, E. (1990) The influence of bulk composition on the speciation of water in silicate glasses. Contributions to Mineralogy and Petrology, 104, 142–162.

Sisson, T.W. and Layne, G.D. (1992) H_2O in basalt and basaltic andesite glass inclusions from four subduction-related volcanoes. Earth and Planetary Science Letters, 117, 619–635.

Vennemann, T.W. and O'Neil, J.R. (1993) A simple and inexpensive method of hydrogen isotope and water analyses of minerals and rocks based on zinc reagent. Chemical Geology, 103, 227–234.

MANUSCRIPT RECEIVED FEBRUARY 10, 1997
MANUSCRIPT ACCEPTED AUGUST 26, 1997